International Journal of Advanced Research in Biological Sciences
ISSN: 2348-8069
www.ijarbs.com
(A Peer Reviewed, Referred, Indexed and Open Access Journal)
DOI: 10.22192/ijarbs Coden: IJARQG (USA) Volume 13, Issue 8 - 2026

Research Article

DOI: http://dx.doi.org/10.22192/ijarbs.2026.13.08.009

# A Sustainable Crab-Shell-Waste-Derived Bio-Composite for Lead Removal and Antimicrobial Activity

**Ms. Lubna S. Majgaonkar[1], Dr. Rupinder Kaur[2], Dr. Surajit Some[3]**

G.N. Khalsa College Matunga Mumbai [1],
Prof. G.N. Khalsa College, Matunga Mumbai[2],
UGC Assistant Professor, Department of Specialty Chemicals Technology (ICT), Mumbai.[3]
Corresponding author E-mail: *lubna.siraj@gnkhalsa.edu.in*

## Abstract

Lead (Pb(II)) contamination in water is a significant environmental and public-health concern due to its persistence, toxicity, and bio-accumulative nature. In this study, a rice-husk derived activated carbon–crab-shell derived calcium carbonate–polypyrrole (AC/$CaCO_3$/PPy) bio-composite was synthesized through acid carbonization and in situ oxidative polymerization and evaluated for Pb(II) removal from aqueous solution. The adsorbent was characterized using FTIR, SEM, and TEM to investigate its functional groups and surface morphology.Batch adsorption experiments were conducted to examine the effects of contact time, solution pH, adsorbent dosage, and initial Pb(II) concentration. The Pb(II) concentrations before and after adsorption were determined using ICP–AES. The optimum adsorbent dosage was 100 mg, achieving 99.36% Pb(II) removal at 60 min. Increasing the initial Pb(II) concentration from 25 to 100 mg/L increased the adsorption capacity from 24.15 to 63.48 mg/g, while removal efficiency decreased from 96.58 to 63.48%. The Kinetic analysis using pseudo-first-order and pseudo-second-order models showed that the PSO model provided the better fit, indicating its suitability for describing Pb(II) adsorption kinetics. The composite demonstrated antimicrobial activity, with inhibition zones of 13 mm against E. coli and 14 mmagainst *S. aureus*, indicating its potential for dual-function wastewater remediation. Overall, the synthesized bio-composite demonstrated promising potential for Pb(II)-contaminated water treatment and antimicrobial applications.

**Keywords:** Pb(II) adsorption; Rice husk activated carbon; Crab-shell calcium carbonate; Polypyrrole; Bio-composite; Heavy-metal removal; Water treatment.

# 1. Introduction

Heavy-metal pollution in water is a serious environmental and public-health issue, arising from activities such as industrial operations, mining, electroplating, battery production, textile processing, and the release of inadequately treated wastewater. Because heavy metals are persistent and non-biodegradable, they can accumulate in aquatic environments and threaten ecosystems and human health (Meftah et al., 2025; Mustapha et al., 2025; Zaimee et al., 2021). Lead [Pb(II)] is of particular concern because of its widespread use in various industrial applications and its harmful effects on human health and the environment. Prolonged exposure may cause neurological, renal, cardiovascular, reproductive, and developmental disorders, especially in children (EPA, 2023; WHO, 2025; Alhashemi & Al-Obaidy, 2025; Bashir et al., 2019). According to the Indian Standard for drinking water, IS 10500:2012, the acceptable lead limit is 0.01 mg $L^{-1}$ (10 µg $L^{-1}$), with no relaxation permitted (Bureau of Indian Standards, 2012). Traditional approaches for removing Pb(II) from contaminated water, such as precipitation, ion exchange, membrane-based separation, reverse osmosis, coagulation–flocculation, electrochemical processes, and solvent extraction, can be associated with drawbacks including high operating costs, substantial energy requirements, membrane fouling, and the production of secondary sludge. Adsorption is therefore widely investigated because of its simplicity, effectiveness, low energy requirement, and economic feasibility (Bashir et al., 2019; Meftah et al., 2025; Singh et al., 2021; Zaimee et al., 2021). The waste-derived adsorbents offer a sustainable alternative for water treatment (Meftah et al., 2025; Mustapha et al., 2025; Singh et al., 2021).

Rice-husk-derived activated carbon provides a porous structure and silica-containing functional groups that promote Pb(II) adsorption through ion exchange and surface complexation (Li et al., 2024; Singh et al., 2021; Zaimee et al., 2021). The crab-shell waste contains calcium carbonate and other functional components that provide adsorption sites while supporting marine-waste valorisation (Triunfo et al., 2024; Alhashemi& Al-Obaidy, 2025; Meftah et al., 2025). Polypyrrole further enhances metal-ion interactions through its chemical stability and nitrogen-containing groups (Maity et al., 2021; Liu et al., 2020; Zhong et al., 2021). Accordingly, this study synthesizes

and evaluates a rice-husk activated carbon–crab-shell calcium carbonate–polypyrrole bio-composite for Pb(II) removal, investigating pH, contact time, dosage, concentration, temperature, kinetics, and equilibrium behaviour.

## 2. Materials and Methodology

The Rice husk and crab shells were collected from a local granary and fish market, respectively, washed, dried, and ground into fine powders. The Synthesis employed a borosilicate beaker, magnetic stirrer, ice bath, analytical balance, measuring cylinders, filter paper, UV–Vis spectrophotometer, and hot-air oven. The Antimicrobial activity was evaluated using sterile Petri plates, nutrient agar, micropipettes, cork borer, cotton swabs, autoclave, incubator, and sterile distilled water against recognized strains of Gram-positive Staphylococcus aureus and Gram-negative Escherichia coli. The antimicrobial assay used sterile Petri dishes, test tubes, micropipettes, cotton swabs, a cork borer, measuring cylinders, beakers, and conical flasks.

### 2.1 Chemicals and Reagents

The chemicals and reagents used in this study included pyrrole monomer (99%, Sigma Aldrich), ferric chloride (Merck), concentrated sulphuric acid, Mueller–Hinton broth and Mueller–Hinton agar (MHB and MHA), 0.5 McFarland standard, ethanol, sterile normal saline, and chloramphenicol.

### 2.2 Preparation of the Bio-Composite

The rice husk-derived activated carbon and crab shell-derived calcium carbonate–polypyrrole (AC/$CaCO_3$/PPy) bio-composite was synthesized through acid carbonization followed by in situ oxidative polymerization. Briefly, 3 g of washed and dried rice husk was carbonized using 50 mL of concentrated $H_2SO_4$ and immediately diluted with 500 mL of distilled water to prevent over-carbonization. Subsequently, 3 g of powdered crab shell was incorporated into the carbonized rice husk suspension and stirred for 3 h at room temperature. The reaction mixture was then cooled to 0–5 °C, followed by the addition of 29 mL of 3 M $FeCl_3$ as the oxidizing agent and 3 mL of pyrrole monomer. In situ polymerization was carried out under continuous stirring for 16 h. The resulting bio-composite was recovered by filtration, thoroughly washed with distilled water until neutral pH was attained, dried at 60 °C for 24 h, and stored in an airtight

container for subsequent characterization and adsorption studies.

## 2.3 Characterization of the Adsorbent

The synthesized AC/$CaCO_3$/PPy bio-composite was characterized using Fourier-transform infrared spectroscopy (FTIR), scanning electron microscopy (SEM), and transmission electron microscopy (TEM). The FTIR analysis was performed to identify the functional groups present in the composite and examine their possible interactions with Pb(II) ions. The SEM was used to evaluate the surface morphology and porosity, whereas TEM provided information on the particle distribution and nanoscale structure. The adsorption-related changes in the functional groups and surface morphology were also examined after Pb(II) treatment to assess the role of the composite structure in the adsorption process. These characterization techniques provided complementary information regarding the chemical composition, morphology, and structural features of the synthesized AC/$CaCO_3$/PPy bio-composite.

## 2.4 Lead adsorption experiment:

### 2.4.1 Preparation of Heavy Metal Solutions:

A 1000 mg/L Pb(II) stock solution was prepared by dissolving 1.598 g of $Pb(NO_3)_2$ in distilled water and making the volume up to 1 L in a volumetric flask. Working solutions of the required concentrations were prepared by appropriate dilution with distilled water, and their pH was adjusted using dilute HCl or NaOH before the adsorption experiments.

### 2.4.2 Batch Adsorption Experiments and Performance Evaluation

The Batch adsorption studies were conducted to assess the Pb(II)-removal performance of AC/$CaCO_3$/PPy bio-composite. The influence of pH, adsorbent dosage, contact time, initial Pb(II) concentration, and temperature was examined individually while maintaining all other operating conditions constant. Following treatment, the adsorbent was separated by filtration, and the remaining Pb(II) concentration in the filtrate was quantified using inductively coupled plasma–atomic emission spectroscopy (ICP–AES). The adsorption efficiency was determined from the equilibrium

adsorption capacity (qe) and percentage removal calculated from the initial and residual Pb(II) concentrations.

The percentage Pb(II) removal was calculated using the formula:

$$\%\ Removal = \frac{C_0 - C_e}{C_0} \times 100$$

Where:
$C_0$= Initial dye concentration
$C_e$= Equilibrium dye concentration

### 2.4.3 Adsorption Kinetics:

The adsorption kinetics of Pb(II) onto the synthesized bio-composite were investigated using Pb(II) solutions with initial concentrations of 25, 50, 75, and 100 mg/L. For each adsorption experiment, 100 mg (0.1 g) of the bio-composite was added to 100 mL (0.1 L) of Pb(II) solution. The initial Pb(II) concentration ($C_0$) was 25 mg/L for the representative calculation. Samples were collected at predetermined contact times from 0 to 60 min. At each interval, the adsorbent was separated by filtration, and the residual Pb(II) concentration in the filtrate was determined using inductively coupled plasma–atomic emission spectroscopy (ICP–AES).The adsorption capacity at time t ($q_t$) was calculated using:

$$q_t = \frac{(C_0 - \dot{C}_t \cdot)}{m} v$$

where $C_0$ and $C_t$ are the initial and residual Pb(II) concentrations (mg $L^{-1}$), respectively, $V$ is the solution volume (L), and $m$ is the mass of the adsorbent (g).The experimental kinetic data were fitted using the pseudo-first-order and pseudo-second-order models, which are commonly applied to evaluate adsorption-rate behaviour.

The Pseudo-First-Order Kinetic Model is expressed as:

$$\ln(qe - qt) = \ln q_e - k_1\, t$$

where qe (mg $g^{-1}$) is the equilibrium adsorption capacity, qt (mg $g^{-1}$) is the adsorption capacity at time $t$, and $k_1$ ($min^{-1}$) is the pseudo-first-order rate constant.

The Pseudo-Second-Order Kinetic Model is represented by:

$$\frac{t}{qt} = \frac{1}{k_2 q_e^2} + \frac{t}{q_e}$$

where $q_t$= amount of dye adsorbed at time $t$(mg/g), $q_e$= adsorption capacity at equilibrium (mg/g), $k_2$= pseudo-second-order rate constant $(g\ mg^{-1}\ min^{-1})t$= contact time (min).

The kinetic parameters were obtained from the linear plots of the respective equations, and the applicability of each model was evaluated based on the correlation coefficient ($R^2$) and the agreement between the calculated and experimental equilibrium adsorption capacities.

### 2.4.4 Antimicrobial Activity:

The antimicrobial activity of the AC/$CaCO_3$/PPy bio-composite was evaluated against *Staphylococcus aureus* and *Escherichia coli* using the agar well-diffusion method. The Cultures were grown in Mueller–Hinton broth at 37 °C for 24 h, adjusted to 0.5 McFarland turbidity, and diluted to approximately $1 \times 10^6$ CFU/mL. The Standardized suspensions were spread onto Mueller–Hinton agar plates, and 100 µL of the bio-composite suspension was added to two wells per plate. After incubation at 37 °C for 24 h, antimicrobial activity was determined by measuring the inhibition zones in millimetres. The assay conditions were based on current antimicrobial susceptibility-testing recommendations.

## 3. Results and Discussion

### 3.1 FTIR, SEM, and TEM Characterization of the AC/$CaCO_3$/PPy Bio-composite:

FTIR analysis confirmed the formation of the AC/$CaCO_3$/PPy bio-composite and incorporation of its constituent materials. The broad band at approximately 3252 $cm^{-1}$ was assigned to O–H stretching associated with hydroxyl groups and adsorbed moisture, while the band near 1620 $cm^{-1}$ was attributed mainly to aromatic C=C and PPy-associated vibrations. The band at 1371 $cm^{-1}$, together with those at 1200 and 1062 $cm^{-1}$, was associated with C–N, C–O and carbonate-related vibrations. The bands at 823 and 706 $cm^{-1}$ were related to carbonate and aromatic-ring deformation vibrations, consistent with $CaCO_3$-containing materials (Jastrzębska et al., 2022; Rezk et al., 2022). SEM revealed a rough, porous and heterogeneous surface with cavities, agglomerated particles and interconnected channels, whereas TEM showed aggregated quasi-spherical nanoparticles with interparticle voids, confirming the nanoscale morphology (Abdel-Karim et al., 2021; Yan et al., 2023).

These structural and morphological characteristics provide accessible surface sites and support the potential of the AC/$CaCO_3$/PPy composite for Pb(II) adsorption.

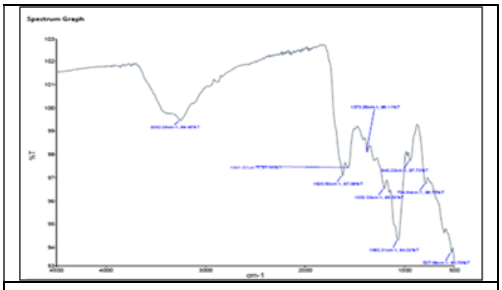

**Figure 1. FTIR – (AC/$CaCO_3$/PPy) Bio-composite**

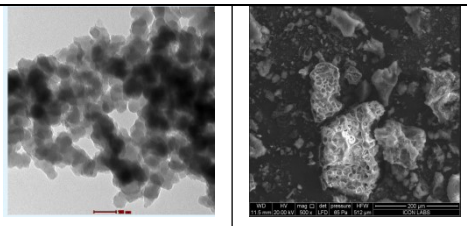

**Fig. 2.a** **Fig. 2.b**

**Fig.2.a SEM image and Fig.2.b TEM image of synthesized AC/$CaCO_3$/PPybio-composite**

## 3.2 Effect of Adsorption Parameters

### 3.2.1 Effect of pH and Contact time on Pb(II) adsorption:

The results indicate that **pH and contact time influenced Pb(II) adsorption capacity and removal efficiency,** reflecting the effects of solution chemistry and interaction time (Al-Tohamy et al., 2022; Yan et al., 2023). At **pH6**, both parameters generally decreased with increasing contact time. At **pH 7.5**, adsorption capacity and removal efficiency increased up to **20 min,** reaching **41.52 mg/g** and **83.04%,** respectively, followed by fluctuations. These pH-dependent

changes may be related to surface charge, proton competition, and Pb(II) speciation (Li et al., 2024; Rezk et al., 2022). **pH 8.5** showed the most favourable and stable performance, with adsorption capacity around **40–50 mg/g** and removal efficiency mostly above **96%** (Abdel-Karim et al., 2021; Yan et al., 2023). The highest values occurred at **50 min**, with **49.91 mg/g** adsorption capacity and **99.81% removal efficiency**. Contact-time effects are associated with the availability and progressive occupation of adsorption sites (Al-Tohamy et al., 2022; Ahmed et al., 2023). Overall, **pH 8.5 was the most favourable condition**, while contact time showed a pH-dependent effect.

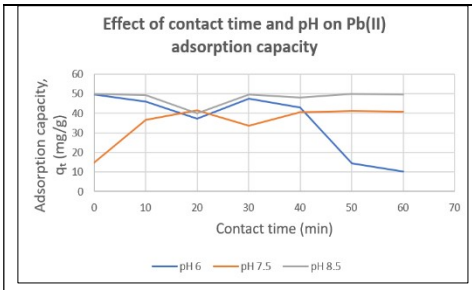


**Fig. 3. Effect of pH and Contact time on Pb(II) adsorption capacity**

### 3.2.2 Effect of Adsorbent Dosage and Contact Time on Pb(II) Adsorption:

The effects of adsorbent dosage and contact time on Pb(II) removal were evaluated at an initial concentration of 50 mg/L using dosages of 80, 100, and 120 mg. At 80 mg, removal increased to 99.68% at 20 min, corresponding to an adsorption capacity of 39.87 mg/g, followed by fluctuations and a final removal of 94.59% and capacity of 37.84 mg/g at 60 min. At 100 mg, Pb(II) removal remained consistently high, reaching 99.81% at 50 min and 99.36% at 60 min, while adsorption capacity ranged from 48.19–49.91 mg/g, with the maximum at 50 min. At 120 mg, removal gradually increased from 47.82% at 10 min to 72.60% at 60 min, while adsorption capacity increased from 28.69 to 43.56 mg/g. The influence of dosage is generally associated with the availability of additional active adsorption sites, whereas contact

time affects progressive occupation of these sites (Al-Khafaji et al., 2020; Bashir et al., 2021; Rezk et al., 2022). Excessive adsorbent dosage may also promote particle aggregation and reduce effective site utilization (Li et al., 2022). Overall, 100 mg provided the highest and most consistent Pb(II) removal and adsorption capacity and was therefore selected as the optimum dosage under the investigated conditions.

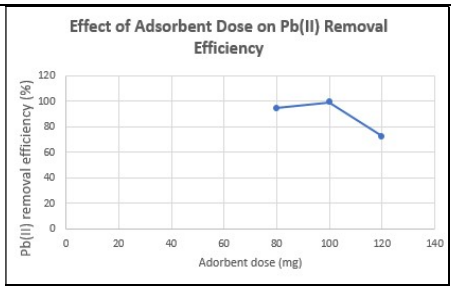


**Fig. 4. Effect of Adsorbent Dose on Pb(II) Removal Efficiency**

### 3.2.3 Effect of Initial Pb(II) Concentration on Pb(II) Adsorption:

The effect of initial Pb(II) concentration on the adsorption performance of the synthesized bio-composite was evaluated at 25, 50, 75, and 100 mg/L. At 60 min, adsorption capacity increased from 24.15 mg/g at 25 mg/L to 40.88, 60.30, and 63.48 mg/g at 50, 75, and 100 mg/L, respectively. This increase can be attributed to the greater concentration gradient and enhanced mass-transfer driving force at higher Pb(II) concentrations, which promote transport of Pb(II) toward available adsorption sites (Wang et al., 2023; Zhang et al., 2021).In contrast, the removal efficiency decreased from 96.58% at 25 mg/L to 81.77%, 80.39%, and 63.48% at 50, 75, and 100 mg/L, respectively. The lower percentage removal at higher concentrations is associated with the limited number of available binding sites relative to the increasing Pb(II) concentration (Al-Khafaji et al., 2020; Khalil et al., 2023). Thus, higher initial Pb(II) concentrations enhanced the adsorption capacity, but reduced the percentage removal because the available adsorption sites became progressively saturated.

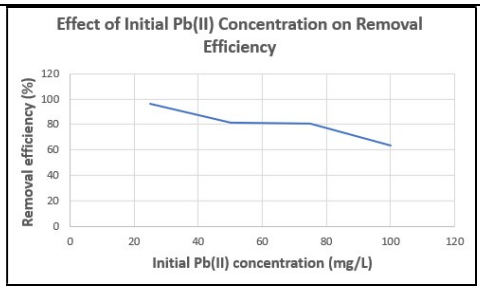


**Fig. 5 Effect of Initial Pb(II) Concentration on Removal Efficiency**

### 3.2.4 Adsorption Kinetics:

The adsorption kinetics of Pb(II) onto the AC/$CaCO_3$/PPy bio-composite were evaluated using the pseudo-first-order (PFO) and pseudo-second-order (PSO) models. The PFO model showed variable agreement with the experimental data, with $R^2$ values of 0.5971–0.9775, while its calculated equilibrium capacities (7.226–29.631 mg $g^{-1}$) differed substantially from the experimental values (24.145–63.476 mg $g^{-1}$), indicating limited applicability. Similar differences between calculated and experimental capacities have been reported for Pb(II) adsorption systems (Wang et al., 2021; Li et al., 2022). In contrast, the PSO model showed excellent correlation ($R^2$ = 0.9943–0.9989), with calculated $q_e$ values (24.155–65.789 mg $g^{-1}$) closely matching the experimental values, particularly at 25 and 75 mg $L^{-1}$. Comparable superiority of the PSO model has been reported for Pb(II) adsorption using biochar and polymer-based adsorbents (Zhang et al., 2021; Al-Khafaji et al., 2023). The highest correlation in the present study was obtained at 100 mg $L^{-1}$ ($R^2$ = 0.9989). Overall, the higher $R^2$ values and closer agreement between calculated and experimental $q_e$ values demonstrate that the PSO model provided the more appropriate description of Pb(II) adsorption kinetics under the investigated conditions.

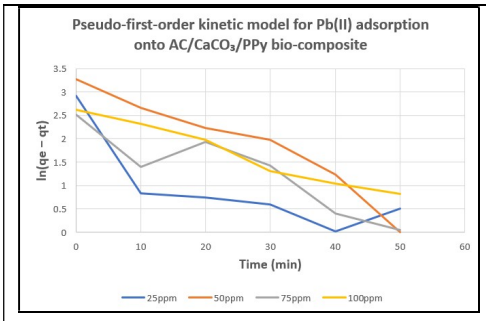


**Fig. 6.a. Pseudo-First-Order Kinetic Model**

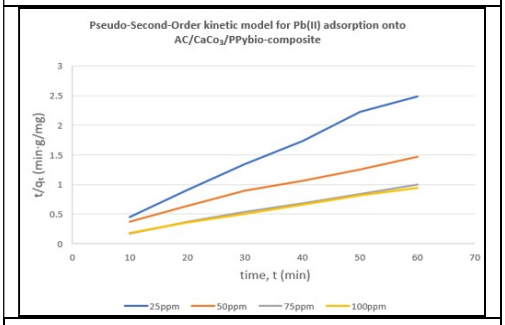


**Fig. 6.b. Pseudo-Second-Order Kinetic Model**

**Table 1. Kinetic Parameters for Pb(II) Adsorption on AC/$CaCO_3$/PPy Bio-composite**

| Initial concentration (mg/L) | Experimental ($q_e$) | PFO ($q_e$) | PFO ($R^2$) | PSO ($q_e$) | PSO ($R^2$) | Best model |
|---|---|---|---|---|---|---|
| 25 | 24.145 | 7.226 | 0.5971 | 24.155 | 0.9955 | PSO |
| 50 | 40.884 | 29.631 | 0.9402 | 46.729 | 0.9943 | PSO |
| 75 | 60.295 | 11.265 | 0.8402 | 62.112 | 0.998 | PSO |
| 100 | 63.476 | 14.073 | 0.9775 | 65.789 | 0.9989 | PSO |

### 3.2.5 Antimicrobial Activity

The antibacterial activity of the synthesized AC/$CaCO_3$/PPy bio-composite was evaluated against *Staphylococcus aureus* and *Escherichia coli* using the agar well diffusion method. The composite produced inhibition zones of 14 mm against *S. aureus* and 12 mm against E. coli, demonstrating antibacterial activity against both Gram-positive and Gram-negative bacteria. In agar diffusion assays, the inhibition zone represents the area of suppressed microbial growth surrounding the test material and provides a qualitative indication of antimicrobial activity (Balouiri et al., 2019; Sadeghi et al., 2022).

The slightly larger inhibition zone against *S. aureus* suggests greater sensitivity of this strain under the present experimental conditions. This difference may be related to variations in bacterial envelope structure: Gram-positive bacteria possess a thick peptidoglycan layer, whereas E. coli has a thinner peptidoglycan layer together with an additional outer membrane that acts as a permeability barrier (Sun et al., 2022; Nikaido, 2020). The antibacterial effect may also be associated with the polypyrrole component, as PPy-containing materials have demonstrated activity against both E. coli and S. aureus (Maruthapandi et al., 2021). Overall, the observed inhibition zones indicate that the AC/$CaCO_3$/PPy bio-composite possesses antibacterial potential in addition to its Pb(II)-adsorption capability, supporting its potential as a multifunctional material for environmental applications.

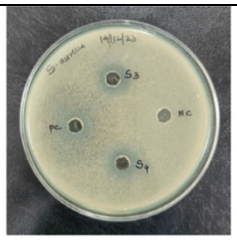

**Fig. 7.a**

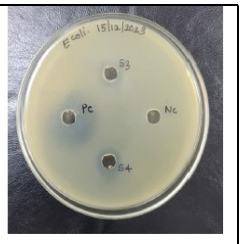

**Fig. 7.b**

**Fig. 7. Agar well diffusion assay against (a) *S. aureus* and (b) *E. coli*.**

### 3.2.6 Adsorption Mechanism and Overall Findings:

Pb(II) removal by the AC/$CaCO_3$/PPy bio-composite proceeds via film diffusion, surface interaction, and intraparticle diffusion (Mostafa et al., 2022). Pb(II) ions migrate from bulk solution to the adsorbent surface, where electrostatic attraction to negatively charged functional groups initiates uptake. Ion exchange with surface ions, coordination with amino, hydroxyl, and other O/N-containing groups, and surface complexation on active sites further strengthen binding, while diffusion into the porous interior enhances capacity.

Adsorption was rapid initially due to abundant sites and a high concentration gradient, reaching optimum performance at 30 min with only minor fluctuations thereafter. Kinetic data fitted the pseudo-second-order model better than the pseudo-first-order model, indicating chemisorption as the dominant mechanism (Li et al., 2019; Tan & Hameed, 2022; Mostafa et al., 2022). Overall, Pb(II) adsorption is governed by electrostatic attraction, ion exchange, coordination, and surface complexation involving oxygen- and nitrogen-containing groups in the composite.

In addition to adsorption, the bio-composite exhibited notable antibacterial activity, attributable to nitrogen-rich polypyrrole moieties, basic calcium carbonate sites, and a positively charged surface capable of interacting with and disrupting bacterial cell membranes (Silva et al., 2021; Santos et al., 2025). This dual functionality suggests potential for simultaneous mitigation of microbial contamination and heavy-metal removal in wastewater treatment. The results confirm the AC/$CaCO_3$/PPy bio-composite as a promising, low-cost adsorbent for Pb(II) removal from aqueous solutions with practical applicability in wastewater treatment.

## 4. Conclusion

The synthesized rice-husk activated carbon–$CaCO_3$–polypyrrole (AC/$CaCO_3$/PPy) bio-composite showed promising Pb(II) removal from aqueous solution. Adsorption capacity increased with initial Pb(II) concentration, reaching 24.15, 40.88, 60.30, and 63.48 mg/g at 25, 50, 75, and 100 mg/L, respectively, while removal efficiency decreased from 96.58% to 63.48%. The optimum dosage was 100 mg, achieving 99.36% removal at 60 min. Kinetic data fitted the pseudo-second-order model better than the pseudo-first-order model, indicating chemisorption dominance. Overall, the AC/$CaCO_3$/PPy bio-composite represents a promising waste-derived adsorbent for Pb(II)-contaminated water, with inherent antibacterial activity that confers dual functionality for the simultaneous mitigation of heavy-metal and microbial contamination in wastewater treatment applications.

## 5. References


1. Abdel-Karim, A., El-Naggar, M. E., & El-Rafie, M. H. (2021). Facile synthesis and characterization of polypyrrole–iron oxide–seaweed nanocomposite and its exploration for adsorptive removal of Pb(II) from heavy metal bearing water. *Chemosphere, 278*, 130400. https://doi.org/10.1016/j.chemosphere.2021.130400
2. Ahmed, M. B., Zhou, J. L., Ngo, H. H., Guo, W., & Chen, M. (2023). Isotherm and kinetic investigations of sawdust-based biochar modified by ammonia to remove methylene blue from water. *Scientific Reports, 13*, 12772.
3. Al-Khafaji, B. M., Al-Baidhani, J. H., & Al-Doury, N. T. (2020). Evaluation of lead (Pb(II)) removal potential of biochar in a fixed-bed continuous flow adsorption system. *Scientific Reports, 10*, 19726.
4. Al-Khafaji, B. M., Al-Baidhani, J. H., & Al-Doury, N. T. (2023). Qualitative and quantitative study on $Pb^{2+}$ adsorption by biochar in solution. *Journal of Chemical Industry and Engineering (China), 74*(2), 830–840. https://doi.org/10.11949/0438-1157.20221299
5. Al-Khafaji, B. M., et al. (2020). A promising and cost-effective biochar adsorbent derived from jujube pit for the removal of Pb(II) from aqueous solution. *Scientific Reports, 10*, 14245. https://doi.org/10.1038/s41598-020-64191-1
6. Al-Tohamy, R., Ali, S. S., Li, F., Okasha, K. M., Mahmoud, Y. A.-G., Elsamahy, T., Jiao, H., Fu, Y., & Sun, J. (2022). A critical review on the treatment of dye-containing wastewater: Ecotoxicological and health concerns of textile dyes and possible remediation approaches for environmental safety. *Ecotoxicology and Environmental Safety, 231*, 113160.
7. Alhashemi, A. S., & Al-Obaidy, A. H. M. (2025). Heavy metal contamination: Sources, health impacts, and mitigation strategies. *Environmental Science and Pollution Research, 32*(15), 1–18.
8. Balouiri, M., Sadiki, M., & Ibnsouda, S. K. (2019). Methods for in vitro evaluating antimicrobial activity: A review. *Journal of Pharmaceutical Analysis, 6*(2), 71–79. https://doi.org/10.1016/j.jpha.2015.11.005
9. Bashir, A., Basha, C. A., & Murthy, Z. V. P. (2019). A review on the removal of lead from aqueous solutions by adsorption. *Environmental Chemistry Letters, 17*(3), 1023–1045.

10. Bashir, S., Zhu, J., Fu, Q., & Hu, H. (2021). A novel, recyclable magnetic biochar modified by chitosan–EDTA for the effective removal of Pb(II) from aqueous solution. *RSC Advances, 11*, 17499–17513.
11. Bureau of Indian Standards. (2012). *IS 10500:2012 Drinking water specification* (2nd rev.). BIS.
12. EPA. (2023). *Integrated science assessment for lead* (January 2024). U.S. Environmental Protection Agency.
13. Jastrzębska, A. M., Sztorch, B., & Radecka, M. (2022). Turning seashell waste into electrically conductive particles. *Materials, 15*(13), 4489. https://doi.org/10.3390/ma15134489
14. Khalil, U., et al. (2023). Removal of toxic lead from aqueous solution using a low-cost adsorbent. *Scientific Reports, 13*, 3442.
15. Li, X., et al. (2022). Use of eggshell-catalyzed biochar adsorbents for Pb removal from aqueous solution. *Materials, 15*, 4386. https://doi.org/10.3390/ma15134386
16. Li, X., Wang, Y., & Zhang, L. (2024). Rice husk-derived activated carbon for heavy metal removal: Mechanisms and applications. *Journal of Environmental Management, 352*, 119876.
17. Li, Y., et al. (2019). Efficient adsorption of lead (II) from aqueous phase solutions using polypyrrole-based activated carbon. *Journal of Environmental Chemical Engineering, 7*(4), 103245.
18. Liu, Y., et al. (2020). Polypyrrole-based composites for heavy metal adsorption: Mechanisms and applications. *Chemical Engineering Journal, 395*, 125123.
19. Maity, S., Dubey, A., & Chakraborty, S. (2021). A review on polypyrrole-coated bio-composites for the removal of heavy metal traces from waste water. *Journal of Industrial Textiles, 51*(2), 1234–1256.
20. Maruthapandi, M., Saravanan, A., Manoj, S., Luong, J. H. T., & Gedanken, A. (2021). Facile ultrasonic preparation of a polypyrrole membrane as an absorbent for efficient oil-water separation and as an antimicrobial agent. *Ultrasonics Sonochemistry, 78*, 105746. https://doi.org/10.1016/j.ultsonch.2021.105746
21. Meftah, S., et al. (2025). Heavy metal polluted water: Effects and sustainable treatment approaches. *Discover Water, 5*(1), 1–24.
22. Mostafa, N. G., Yunnus, A. F., Elawwad, A., &Kyzas, G. (2022). Adsorption of Pb(II) from water onto ZnO, $TiO_2$, and $Al_2O_3$: Process study, adsorption behaviour, and thermodynamics. *Journal of Chemistry, 2022*, 7582756.
23. Mustapha, L. S., et al. (2025). A comprehensive review on potential heavy metals in the environment and their remediation. *Environmental Research, 268*, 120456.
24. Nikaido, H. (2020). Porins and small-molecule translocation across the outer membrane of Gram-negative bacteria. *Nature Reviews Microbiology, 18*, 164–176. https://doi.org/10.1038/s41579-019-0294-2
25. Rezk, R. A., Abdel-Salam, Z., Abdel Ghany, N. A., Abdelkreem, M., & Abdel-Harith, M. (2022). LIBS and pXRFvalidation for the removal of Pb by bio-$CaCO_3$ nanoparticles from contaminated water. *SN Applied Sciences, 4*, 151. https://doi.org/10.1007/s42452-022-05014-y
26. Sadeghi, A., et al. (2022). A review of commonly used methodologies for assessing the antibacterial activity of honey and honey products. *Foods, 11*.
27. Santos, R. O., et al. (2025). Light-mediated antibacterial activity of composites of polypyrrole and zinc oxide nanoparticles. *Materials, 18*(18), 4123.
28. Silva, M. A., et al. (2021). Antibacterial activity of polypyrrole-based nanocomposites: A mini-review. *Polímeros, 31*(1), e20210012.
29. Singh, R., et al. (2021). Adsorption technologies for heavy metal removal from wastewater: A review. *Journal of Water Process Engineering, 44*, 102345.
30. Sun, J., Rutherford, S. T., Silhavy, T. J., & Huang, K. C. (2022). Physical properties of the bacterial outer membrane.

*Nature Reviews Microbiology, 20*, 236–248. https://doi.org/10.1038/s41579-021-00638-0
31. Tan, K. L., & Hameed, B. H. (2022). Second or pseudo-second-order model for adsorption kinetics? *Separation Science and Technology, 57*(10), 1623–1635.
32. Triunfo, R., et al. (2024). Valorization of crab shell waste as adsorbents for heavy metal removal. *Waste Management, 178*, 456–467.
33. Wang, J., et al. (2021). One-pot synthesis of spherical nanoscale zero-valent iron/biochar composites for efficient removal of Pb(II). *RSC Advances, 11*, 34772–34784. https://doi.org/10.1039/D1RA07373G
34. Wang, J., et al. (2023). Removal of Pb(II) from aqueous solution and adsorption kinetics of corn stalk biochar. *Processes, 11*(8), 2438.
35. WHO. (2025). *Exposure to lead: A major public health concern*. World Health Organization.
36. Yan, L., et al. (2023). Mg-doped $CaCO_3$ nanoarchitectures assembled by high-index facets for efficient trace removal of Pb(II). *Rare Metals*. https://doi.org/10.1007/s12598-022-02181-0
37. Zaimee, N. A., et al. (2021). Adsorption of heavy metals using low-cost adsorbents: A review. *Journal of Environmental Chemical Engineering, 9*(5), 105678.
38. Zhang, Y., et al. (2021). Characteristics and mechanism of $Pb^{2+}$ adsorption from aqueous solution onto biochar derived from microalgae and chitosan-modified microalgae. *Frontiers in Environmental Chemistry, 2*, 693509. https://doi.org/10.3389/fenvc.2021.693509
39. Zhong, Q., et al. (2021). Polypyrrole-functionalized adsorbents for heavy metal removal: Synthesis and mechanisms. *Journal of Hazardous Materials, 403*, 123890.

**Access this Article in Online**

Website: www.ijarbs.com

Subject: Ecotoxicology

Quick Response Code

DOI:10.22192/ijarbs.2026.13.08.009

How to cite this article:
Lubna S. Majgaonkar, Rupinder Kaur, Surajit Some. (2026). A Sustainable Crab-Shell-Waste-Derived Bio-Composite for Lead Removal and Antimicrobial Activity. Int. J. Adv. Res. Biol. Sci. 13(8): 111-125.
DOI: http://dx.doi.org/10.22192/ijarbs.2026.13.08.009